



Research paper

In situ $^{13}\text{CO}_2$ pulse labelling of field-grown eucalypt trees revealed the effects of potassium nutrition and throughfall exclusion on phloem transport of photosynthetic carbon

Daniel Epron^{1,2,3,10}, Osvaldo Machado Rodrigues Cabral⁴, Jean-Paul Laclau^{3,5,6}, Masako Dannoura⁷, Ana Paula Packer⁴, Caroline Plain^{1,2}, Patricia Battie-Laclau⁸, Marcelo Zacharias Moreira⁸, Paulo Cesar Ocheuze Trivelin⁸, Jean-Pierre Bouillet^{3,6}, Dominique Gérant^{1,2} and Yann Nouvellon^{3,9}

¹UMR 1137, Ecologie et Ecophysiologie Forestières, Faculté des Sciences, Université de Lorraine, F-54500 Vandoeuvre-les-Nancy, France; ²INRA, UMR 1137, Ecologie et Ecophysiologie Forestières, Centre de Nancy, F-54280 Champenoux, France; ³CIRAD, UMR Eco&sols, Ecologie Fonctionnelle & Biogéochimie des Sols & Agro-écosystèmes, F-34060 Montpellier, France; ⁴Embrapa Meio Ambiente, CEP 13820-000, Jaguariúna, São Paulo, Brazil; ⁵Universidade Estadual de São Paulo, Botucatu, CEP 18610-300 São Paulo, Brazil; ⁶Departamento de Ciências Florestais, ESALQ, Universidade de São Paulo, ESALQ, CEP 13418-900 Piracicaba, São Paulo, Brazil; ⁷Laboratory of Forest Utilization, Department of Forest and Biomaterial Science, Graduate School of Agriculture, Kyoto University, Kyoto 606-8502, Japan; ⁸Centro de Energia Nuclear na Agricultura, Universidade de São Paulo, CEP 13400-970 Piracicaba, São Paulo, Brazil; ⁹Departamento de Ciências Atmosféricas, IAG, Universidade de São Paulo, ESALQ, CEP 05508-900 São Paulo, Brazil; ¹⁰Corresponding author (daniel.epron@univ-lorraine.fr)

Received April 21, 2015; accepted August 10, 2015; published online September 30, 2015; handling Editor Peter Millard

Potassium (K) is an important limiting factor of tree growth, but little is known of the effects of K supply on the long-distance transport of photosynthetic carbon (C) in the phloem and of the interaction between K fertilization and drought. We pulse-labelled 2-year-old *Eucalyptus grandis* L. trees grown in a field trial combining K fertilization (+K and -K) and throughfall exclusion (+W and -W), and we estimated the velocity of C transfer by comparing time lags between the uptake of $^{13}\text{CO}_2$ and its recovery in trunk CO_2 efflux recorded at different heights. We also analysed the dynamics of the labelled photosynthates recovered in the foliage and in the phloem sap (inner bark extract). The mean residence time of labelled C in the foliage was short (21–31 h). The time series of ^{13}C in excess in the foliage was affected by the level of fertilization, whereas the effect of throughfall exclusion was not significant. The velocity of C transfer in the trunk ($0.20\text{--}0.82\text{ m h}^{-1}$) was twice as high in +K trees than in -K trees, with no significant effect of throughfall exclusion except for one +K -W tree labelled in the middle of the drought season that was exposed to a more pronounced water stress (midday leaf water potential of -2.2 MPa). Our results suggest that besides reductions in photosynthetic C supply and in C demand by sink organs, the lower velocity under K deficiency is due to a lower cross-sectional area of the sieve tubes, whereas an increase in phloem sap viscosity is more likely limiting phloem transport under drought. In all treatments, 10 times less ^{13}C was recovered in inner bark extracts at the bottom of the trunk when compared with the base of the crown, suggesting that a large part of the labelled assimilates has been exported out of the phloem and replaced by unlabelled C. This supports the 'leakage-retrieval mechanism' that may play a role in maintaining the pressure gradient between source and sink organs required to sustain high velocity of phloem transport in tall trees.

Keywords: carbon isotope, carbon transfer, drought, *Eucalyptus grandis*, fertilization.

Introduction

Potassium (K) is an important limiting factor of crop and forest productivity (Tripler et al. 2006, Pettigrew 2008, Römhild and

Kirkby 2010, Sardans and Peñuelas 2015), especially on highly weathered tropical soils (Cakmak 2010, Cobo et al. 2010, Taulya 2013). Potassium availability has a major influence on

the growth of tropical trees (Laclau et al. 2009, Wright et al. 2011, Epron et al. 2012b, Santiago et al. 2012). However, as for other nutrients, it is still unclear whether growth reduction for K-deficient trees results primarily from a decrease in carbon (C) supply through photosynthesis or from direct effects on tissue growth (Fatichi et al. 2014).

Temporal patterns in symptoms of K deficiency on *Pinus radiata* D. Don needles indicate possible interactive effects of K and water availability (Smethurst et al. 2007). Strong interactions between water and K limitations on light interception, gross primary productivity and light use efficiency in eucalypt plantations were confirmed using a modelling approach (Christina et al. 2015). Drought stress is often associated with a disturbance in intracellular K⁺ homeostasis because drought both enhances K requirements and decreases K uptake (Oddo et al. 2014, Shabala and Pottosin 2014). It has often been suggested that K fertilization may thus alleviate the adverse effects of water stress (Robin et al. 1989, Taulya 2013), provided that the positive effect on stomatal regulation is not offset later on by a higher water use exposing trees to a more rapid soil water depletion (Battie-Laclau et al. 2014b).

Potassium is indeed a key actor of stomatal regulation (Fischer 1968, Talbott and Zeiger 1996, Roelfsema and Hedrich 2005), and it also contributes to osmotic adjustment and turgor-related cell elongation (Triboulot et al. 1997, Shabala and Lew 2002, Wind et al. 2004, Fromm 2010, Battie-Laclau et al. 2013). Potassium also regulates the xylem hydraulic conductance in trees (Oddo et al. 2011, Nardini et al. 2012), and K fertilization reduces the occurrence of drought-induced xylem embolism (Trifilò et al. 2011). Net CO₂ assimilation was enhanced in K-fertilized *Eucalyptus grandis* L. trees, not only as a result of higher leaf area and lower diffusional limitations (higher stomatal and mesophyll conductance) but also as a consequence of higher chlorophyll contents and higher maximum rates of electron transport and carboxylation (Battie-Laclau et al. 2013, 2014a, 2014b). These results were in agreement with previous observations on hickory seedlings and almond trees, showing that non-stomatal limitation of photosynthesis occurred in response to K deficiency (Basile et al. 2003, Jin et al. 2011). Potassium ions may also alleviate the effect of dehydration on chloroplast photosynthesis (Berkowitz and Whalen 1985, Pier and Berkowitz 1987). At the whole-tree level, the effect of K supply on eucalypt growth is related to an effect not only on C acquisition but also on drastic changes in C allocation (Epron et al. 2012b). Growth partitioning among the different tree compartments is mediated by the long-distance transport of carbohydrates from source (mainly foliage for fast-growing evergreen tropical species) to sink organs through the phloem pathway. The role of K supply in phloem loading and photosynthate transport has been well documented some decades ago in several crop species (Hartt 1969, 1970, Mengel and Viro 1974, Mengel and Haeder 1977, Doman and Geiger 1979), but no

study has reported the effect of K supply on phloem dimension and anatomy. It was recently shown that voltage-gated K channels are involved in the reuptake of sucrose leaking from the phloem (Gajdanowicz et al. 2011), suggesting that K supply may play a crucial role in supporting phloem transport because unloading and reloading sucrose may help to maintain the pressure gradient between source and sink organs (De Schepper et al. 2013b).

Because phloem transport is a mass flow osmotically driven by the hydrostatic gradient between source and sink organs involving transfer of water between xylem and phloem (the Münch hypothesis, Minchin and Lacointe 2005, Knoblauch and Peters 2010, Stroock et al. 2014), the photosynthate transport rate might be influenced by water availability (Nikinmaa et al. 2014, Sevanto 2014). A decrease in xylem water potential requires an increase in solute concentration in the phloem, which potentially increases phloem viscosity, reducing the rate of transport (Woodruff 2014), except if K contributes to the required increase in osmotic pressure (Lang 1983). Similar to K deficiency, water stress also reduces the rate of C translocation (Sung and Krieg 1979, Deng et al. 1990a, 1990b, Ruehr et al. 2009). However, as far as we are aware, the effects of K supply on the long-distance transport of photosynthetic C in the phloem and the interaction between K fertilization and drought have never been investigated in field-grown trees.

Our study aimed to assess the effect of K deficiency and water deficit on phloem transport of photosynthates in *E. grandis* trees growing in a field experimental trial combining K fertilization and throughfall exclusion. We hypothesized that the velocity of C transfer is lower in K-deficient than in K-supplied trees and that K nutrition and water availability interactively influence this velocity. To test this hypothesis, we estimated the velocity of C transfer by comparing time lags between the uptake of ¹³CO₂ and its recovery in trunk CO₂ efflux recorded at different heights along the trunk and in roots, and we analysed the dynamics of the labelled photosynthates recovered in the foliage and in inner bark extracts.

Materials and methods

Study site and experimental design

The study was conducted on eucalypt trees (*E. grandis*) at the Itatinga experimental station of the University of São Paulo in Brazil (23°02'S, 48°38'W, 850 m elevation) where soils are deep ferralsols developed on Cretaceous sandstone (Laclau et al. 2010). Mean annual air temperature and precipitation were 20 °C and 1360 mm, respectively, over the last 15 years.

A split-plot experimental design was set up with six treatments (three fertilization crossed with two water supply regimes) in three blocks (Battie-Laclau et al. 2014b). A single highly productive *E. grandis* clone was planted at a spacing of 2 m × 3 m in June 2010 with 144 individuals per plot (three

buffer rows). All the trees were fertilized with 3.3 g P m^{-2} , 200 g m^{-2} of dolomitic lime and trace elements at planting and with 12 g N m^{-2} at 3 months of age. Other experiments at the same site showed that the amounts of N, P, Ca, Mg and micronutrients applied in our experiment were not limiting the growth of *E. grandis* trees. Four treatments were investigated in our study:

- +K +W: 17.4 g K m^{-2} applied as KCl at age 3 months and no throughfall exclusion;
- +K -W: 17.4 g K m^{-2} applied as KCl at age 3 months and 37% of throughfall excluded;
- K +W: no K addition and no throughfall exclusion;
- K -W: no K addition and 37% of throughfall excluded.

Starting in September 2010, throughfall was partially excluded in the -W plots using panels made of clear glasshouse plastic sheets mounted on wooden frames at a height varying between 1.6 and 0.5 m (Figure 1b). A detail presentation of the experimental setting can be found in Battie-Laclau et al. (2014b). About 500 mm of water was excluded each year from the -W plots.

In May 2012, three dominant trees were selected in one block in each of the four treatments (+K +W, +K -W, -K +W and -K -W). The distribution of cross-sectional areas of all trees in each treatment was divided into thirds of equal range, and the three labelled trees were selected close to the mean of the cross-sectional areas of the trees in the upper third (see Table 1 for the averaged dimension of the selected trees in each treatment). The two first trees of each treatment were labelled between 27 May and 4 June 2012 and the last trees were labelled between 7 August and 10 August 2012, corresponding to the expected beginning and the middle of the dry season, respectively.

Environment and tree monitoring

Volumetric soil water content was measured weekly over the study period with three time-domain reflectometry probes per layer (Trase Soilmoisture, Santa Barbara, CA, USA) installed at depths of 0.15, 0.5, 1.0, 1.5, 3.0, 4.5 and 6.0 m in each treatment. Probes were calibrated by gravimetric soil water content and bulk density measurements. Global radiation, rainfall, air



Figure 1. (a) Large-scale throughfall exclusion experiment at the Itatinga experimental station of the University of São Paulo, Brazil. (b) Cross section of secondary phloem from inner bark strip collected on one +K +W tree, with cambium at the bottom (scale bar = $500 \mu\text{m}$). (c) Crown labelling chamber installed on one eucalypt tree. (d) Ninety-six solenoid valves controlled by six relay controllers and a data-logger used to sequentially monitor isotope composition of respiration chambers with a CO_2 isotope analyser.

Table 1. Circumference at 1.3 m high (C_{130}), tree height (H), sapwood cross-sectional area (A_S), bark cross-sectional area (A_B), leaf area (A_L) and leaf biomass (B_L) of the labelled trees at harvest and crown CO_2 uptake (U), predawn (Ψ_{WP}) and midday (Ψ_{WM}) leaf water potentials and their differences ($\Delta\Psi$) and xylem sap flux (J_W) at the labelling dates. Values are means and their standard errors for three trees per treatment. Effects of K fertilization (F), throughfall exclusion (T) and their interaction were tested using a non-parametric two-way analysis of variance based on the ranks (P -values are shown).

F	T	C_{130} (cm)	H (m)	A_S (cm 2)	A_B (cm 2)	A_L (m 2)	B_L (kg)	Crown U (mmol s $^{-1}$)	Ψ_{WP} (MPa)	Ψ_{WM} (MPa)	$\Delta\Psi$ (MPa)	J_W (l day $^{-1}$)
+K	+W	36.7 ± 0.7	13.3 ± 0.3	62 ± 2	17.8 ± 0.5	26 ± 2	4.0 ± 0.1	0.22 ± 0.02	-0.25 ± 0.07	-1.46 ± 0.10	1.21 ± 0.07	21 ± 2
+K	-W	31.8 ± 0.6	12.6 ± 0.0	49 ± 2	12.2 ± 0.4	19 ± 2	2.9 ± 0.1	0.19 ± 0.01	-0.38 ± 0.06	-1.84 ± 0.18	1.46 ± 0.12	16 ± 1
-K	+W	25.7 ± 0.6	9.6 ± 0.1	33 ± 2	8.5 ± 0.4	21 ± 2	2.7 ± 0.2	0.11 ± 0.02	-0.24 ± 0.08	-1.29 ± 0.10	1.05 ± 0.05	14 ± 1
-K	-W	23.1 ± 0.3	9.7 ± 0.1	28 ± 1	6.5 ± 1.1	11 ± 2	1.5 ± 0.2	0.09 ± 0.00	-0.29 ± 0.07	-1.43 ± 0.03	1.14 ± 0.04	8 ± 1
F effect		0.004	0.004	0.004	0.004	0.02	0.01	0.004	0.52	0.03	0.04	0.006
T effect		0.15	0.63	0.15	0.20	0.05	0.08	0.63	0.23	0.10	0.09	0.11
F × T		1	0.34	1	0.87	1	1	1	0.58	0.52	0.63	1.00

temperature and humidity were measured half-hourly using an automatic station placed on the top of a 21 m tower located 50 m from the experiment.

Predawn leaf water potentials (Ψ_{WP}) were measured from 05:00 to 07:00 h on the labelled trees (the labelling day or the previous day) using a nitrogen gas-supplied pressure chamber (PMS Instrument Company, Albany, OR, USA). Measurements were made on two fully expanded leaves per tree (~2 months old) in the upper third of the canopy at the northern side (sun-exposed) of each tree. Midday leaf water potential (Ψ_{WM}) was measured on another leaf of the same trees (same age and position in the crown) between 12:00 and 14:00 h.

Volumetric xylem sap flux density, which is equivalent to the velocity of water transfer in the trunk (V_W), was measured on all labelled trees using the thermal dissipation method (Granier 1985). Each tree was equipped with two home-made temperature probes at 1.3 m above soil level with 10 cm vertical spacing and at 20 mm depth in the trunk. We assumed that probes measured an integrated instantaneous sap velocity over the average sapwood thickness for instrumented trees. Sap flux sensors were protected from thermal influences and water intrusion by a reflective foil. Sensor output voltage was recorded every 30 s, and the average value was stored every 30 min (CR1000 data- loggers and AM16/32 multiplexers, Campbell Scientific Inc., Logan, UT, USA). The volumetric sap flux density was calculated using a calibration equation established previously for *E. grandis* trees at our study site from direct measurements of water uptake in a bucket for 18 trees (between 18 and 72 months of age) destructively sampled (slope of 0.97 and $R^2 = 0.94$ between predicted and measured values of tree transpiration, J.S. Delgado-Rojas, personal communication). Sap flux density was scaled to whole-tree xylem sap flux (J_W) by multiplying V_W by the sapwood area that was estimated by dye injection in each stem cut at the end of the experiment.

Tree growth in circumference at 1.3 m above soil level was monitored weekly from 26 May 2012 to 5 September 2012 at 0.2 mm resolution on all labelled trees using aluminium dendrometer bands. Bark cross-sectional area of each labelled tree

was estimated from the tree circumference measured above and below the bark at 1.3 m high when the trees were destructively sampled at the end of the experiment. Leaf area was estimated for each tree from measurements of the leaf biomass and specific leaf area (SLA) in three crown sections (lower, middle and upper). Fresh mass of all leaves in the three crown sections was measured in the field, and subsamples were brought back to the laboratory, scanned, oven-dried at 65 °C and weighed.

A bark strip (5 cm length and 1 cm width) was collected at 1.3 m on one tree per treatment (two trees in -K +W) and stored in 3.75% glutaraldehyde in 0.1 M phosphate buffer (pH 7.2). Cross sections of bark strips (40 µm thick) were coloured with safranin, dehydrated by ethanol and xylene and mounted in Canada balsam. Microphotographs were taken with a magnifying power of 100 (Figure 1b). The thickness of phloem tissue from cambium to the outer bark, the number of sieve tubes per unit area of phloem tissue and the cross-sectional area of the sieve tubes were estimated on the central 0.8 mm width part using an image analysis software (ImageJ, version 1.47v; National Institutes of Health, Bethesda, MD, USA). Only well-differentiated and non-collapsed sieve tubes were counted and measured.

Pulse labelling of tree crown

The whole crown of a tree was inserted into a 27 m 3 (trees from -K treatments) or 38 m 3 (trees from +K treatments) chamber made of 300 µm polyane film and held with ropes by a 10–15 m height steel scaffolding set-up around the tree the previous day (Figure 1c). The base of the chamber, made with two stainless steel half-plates with circular openings to accommodate the trunk, was set up at the base of the crown and secured on the scaffolding.

One air conditioner (YORK 9000 BTU/h, Hong Kong, China) and four axial fans were disposed in the labelling chamber to ensure a good mixing of air and to help maintaining air temperature inside the crown labelling chamber ~5 °C above the outside air temperature, which averaged 24.4 ± 0.5 °C during the 12 labelling periods.

Immediately after closing the chamber, the CO₂ concentration inside the labelling chamber was continuously monitored with an infrared gas analyser (LI-840A, LI-COR Industries, Lincoln, NE, USA) that was designed and calibrated for ¹²CO₂ and that exhibited a low sensitivity to ¹³CO₂. The CO₂ concentration decreased linearly by 25–45 µmol mol⁻¹ during the first 5 min after the chamber was closed because of CO₂ uptake by photosynthesis. The slope of this decline was used to calculate in real time the net CO₂ uptake of the crown. The flow rate of pure ¹³CO₂ (99.299%, Cambridge Isotope Laboratory Inc., Andover, MA, USA) was then constantly injected into the labelling chamber for 40 min using a mass flow controller (SLA5860S, Brooks, Hatfield, PA, USA) at a rate adjusted to balance the estimated net rate of CO₂ consumption by crown photosynthesis. The amount of ¹³CO₂ injected ranged from 0.34 to 0.81 mol per tree, depending on the size and the activity of the tree crown. The ¹³CO₂ was delivered in the vicinity of two fans. After the 40-min injection period, the tree was allowed to assimilate most of the remaining ¹³CO₂ in the labelling chamber for an additional 20 min. Then the chamber was rapidly opened and removed. The label duration was thus 60 min for all trees. We opted for short and constant pulse duration to limit biases in our estimation of the rate of transfer and residence times of C in labile pools (Epron et al. 2012a). The labelling was done around noon, starting not earlier than 11:00 h and ending no later than 14:00 h.

¹³C composition of trunk and root CO₂ efflux

The appearance of ¹³C in trunk and root CO₂ effluxes was determined by off-axis integrated cavity output spectroscopy (CCIA-36d, Los Gatos Research, Mountain View, CA, USA). The analyser was connected to 48 chambers (two trunk chambers and two root chambers on each tree). Measurement frequency was changed to make more frequent measurements (every 50 min) during the first 2 days after labelling and less frequent measurements thereafter (every 200 min for two additional days and every 400 min until 7 days after labelling). The analyser sampled the gas in each chamber through 6 mm diameter Tygon plastic tubing for 4 min, including a 1-min purge period before and after the measurement that was initiated by closing the chamber and terminated by opening it. All tubes were 33 m long, which was the longest distance between a chamber and the analyser.

The trunk chambers (height: 10 cm, length: 20 cm and width: 20 cm; i.e., 4 l without trunk) were made of two transparent acrylic parallelepipeds with semi-circular openings to accommodate the trunk. One side on the box was opened and closed automatically with a pneumatic cylinder. Chambers were left open between measurements, and air renewal was ensured by a small electric fan. One chamber was set up just under the crown, ~30 cm below the base of the labelling chamber, from 2.1 to 3.6 m above the soil, depending on the height of the tree. The second chamber was set up at the base of the trunk

just above the soil (0.3 m). The height of each chamber was measured.

The root chambers were set up after carefully removing the soil with a vacuum cleaner down to 20 cm, leaving only the target root segment of the focal tree. An acrylic board was inserted just under the root to limit the contribution of CO₂ diffusing from deeper soil layers (Dannoura et al. 2006). Two holes were cut at the bottom edge of a 20 cm diameter collar to accommodate the root. The collar heights ranged from 14 to 20 cm, depending on the root depth. The collar was sealed with putty on the acrylic board and filled with sand leaving 4.1 ± 0.3 cm of air above the sand (~1.3 l). A mobile lid at the top of the collar was controlled by two pneumatic cylinders to close the chamber during each measurement. The chambers were left open between measurements with lids in vertical position. For each tree, one chamber was set up close to the trunk (0.1–0.3 m away) on a coarse root (20–58 mm in diameter) and the other chamber was set up farther from the trunk (0.4–2.2 m) on another root (6–15 mm in diameter).

Ninety-six solenoid valves (SY5000, SMC Corporation, Tokyo, Japan) were used to switch measurements from one chamber to another (Figure 1d). Another set of 48 solenoid valves was used to control the air flow into each pneumatic cylinder from a gas tank pressurized by an air compressor, allowing the closure of the desired chamber. All the valves were controlled using six relay controllers (SDM-CD16AC, Campbell Scientific Inc.) connected to a data-logger (CR3000, Campbell Scientific Inc.). Air was circulated continuously from the inlet to the outlet of the selected chamber with a membrane pump (KNF Neuberger N86 KNDC, Freiburg, Germany) at a flow rate of 6 l min⁻¹.

After the closure of the chamber, the CO₂ concentration [CO₂] increased linearly and the isotope composition of CO₂ ($\delta^{13}\text{C-CO}_2$) in the chamber decreased or increased depending on whether the initial atmospheric CO₂ was mixed with ¹³C-depleted CO₂ (unlabelled source) or ¹³C-enriched CO₂ (labelled source). The isotope composition of respiration CO₂ was determined as the intercept of the linear relationship between the reciprocal of [CO₂] and $\delta^{13}\text{C-CO}_2$ (Keeling 1958).

Time lags and velocity of C transfer

Due to the low precision achieved by the CCIA-36 device under field conditions (5‰), the estimated isotope composition of respiration CO₂ was used only for detecting the time lag between labelling and the onset of the recovery of labelled CO₂ in the respiratory efflux. The precision of the lag estimates depends on the measurement frequency and was thus 50 min in our experiment.

The velocity of C transfer in trunk (V_C , m h⁻¹) was calculated as

$$V_C = \frac{d}{L_B - L_T} \quad (1)$$

with d (m) the distance between the two trunk chambers and L_T and L_B the lag after labelling estimated for the top chamber (just below the crown, L_T) and for the bottom chamber (at the base of the trunk, L_B). As already noticed, this calculation assumed that delays between the time the labelled carbohydrates arrived at a given position along the trunk and the time they were used for respiration were similar at the two positions, so that they were cancelled by the subtraction of the two lags (Dannoura et al. 2011). It also assumed that the time needed to reach the detection threshold is the same at the two positions along the trunk.

We did not calculate the velocity of C transfer in root because of the short distance between the base of the trunk and the two root chambers. We calculated lag in root as the difference between the onset of the recovery of the labelled C in the respiratory efflux at the base of the trunk and the onset of the recovery of the label in the respiratory efflux in each root chamber. Because the bottom trunk chamber was not at height zero but ~30 cm above the soil, we estimated the time the labelled CO_2 arrived at height zero for each tree knowing the height of the bottom trunk chamber and V_C .

13C composition of bulk leaf organic matter and phloem extracts

Leaves were collected just before the installation of the labelling chamber, within the 20 min following the withdrawal of the labelling chamber, 5 h and 1, 2, 4 and 7 days later. Two leaf samples were collected each time at three positions in the crown that was divided into three equal-length sections (lower, middle and upper). Each sample was made of 12 leaves collected along four branches from the four cardinal directions. The leaf samples were frozen in liquid nitrogen, stored at -20°C , and finally freeze-dried and ground.

Two small disks of bark (12 mm diameter) were collected near the trunk respiration chambers both at the base of the crown (from 2.7 to 4.0 m above the soil) and at the base of the trunk (from 0.1 to 0.3 m above the soil) just before the installation of the labelling chamber, 5 h and 1, 2, 4 and 7 days after labelling. The outer part of the bark was removed and the inner bark tissue was infused in a 10 ml vial containing 2 ml of ultra-pure water for 5 h at ambient temperature. The inner bark extracts were filtrated on nylon cartridges (Whatman, 0.2 μm , diameter 25 mm, ref. 17,463,433) and the filtrates were evaporated at 40°C .

Leaf and inner bark extract samples were weighed in tin capsules and analysed for C isotope composition and total C using an elemental analyser coupled to an isotope ratio mass spectrometer (Europa ANCA-GSL with HYDRA 20-20, Sercon Limited, Crewe, UK, for leaf samples, and CHN-1110, Carlo Erba, Milan, Italy, with Delta Plus, Thermo Scientific, Bremen, Germany, for inner bark extracts).

Calculation of excess ^{13}C

The stable isotope results are expressed according to the nomenclature recommended by the Commission on Isotopic Abundances and Atomic Weights of the International Union of Pure and Applied Chemistry (Coplen 2011). The ^{13}C atom fraction, $x(^{13}\text{C})$, was calculated from the isotope composition $\delta^{13}\text{C}$ with R_{VPDB} the isotope ratio of Vienna Pee Dee Belemnite standard (0.0111802):

$$x(^{13}\text{C}) = \frac{^{13}\text{C}}{^{12}\text{C} + ^{13}\text{C}} = \frac{(\delta^{13}\text{C} + 1) \times R_{\text{VPDB}}}{[(\delta^{13}\text{C} + 1) \times R_{\text{VPDB}}] + 1} \quad (2)$$

Excess ^{13}C , $x^E(^{13}\text{C})$, was calculated after accounting for the background ^{13}C atom fraction measured on the same tree before labelling, $x(^{13}\text{C}_{\text{UN}})$:

$$x^E(^{13}\text{C}) = x(^{13}\text{C}) - x(^{13}\text{C}_{\text{UN}}) \quad (3)$$

$x^E(^{13}\text{C})$ in the whole crown was calculated for each tree at each sampling time as the weighted average of $x^E(^{13}\text{C})$ in leaves collected in the upper, middle and lower parts of the crown, taking into account the distribution of leaf biomass between these three compartments.

Tracer kinetics analysis

The time courses of $x^E(^{13}\text{C})$ within the crown after labelling were described by exponential curves, assuming that (i) the processes involved followed first-order kinetics, (ii) the amount of labelled C was maximal immediately after labelling and (iii) the $x^E(^{13}\text{C})$ disappearance was only governed by tracer efflux (Epron et al. 2012a):

$$x^E(^{13}\text{C})(t) = C_L \times \exp(-k \times t) + C_S \quad (4)$$

C_L was the labile pool of $x^E(^{13}\text{C})$ at time 0, C_S the asymptotic amount of $x^E(^{13}\text{C})$ remaining [$C_L + C_S$ was the total $x^E(^{13}\text{C})$ at time 0] and k the rate of disappearance of $x^E(^{13}\text{C})$ with time (t). The mean residence time of the labile pool of $x^E(^{13}\text{C})$, τ , was the reciprocal of k . The parameters were determined after fitting the model by iteratively minimizing the sum of squared differences between measured and predicted $x^E(^{13}\text{C})$ using the Microsoft Excel solver tool.

Statistics

Because of the low number of replicates ($n = 3$), treatment effects on tree dimension, velocities, fluxes, water potentials and kinetic model parameters were analysed using the conservative Scheirer-Ray–Hare extension of the Kruskal–Wallis test (Sokal and Rohlf 1995), which is a non-parametric two-way analysis of variance based on the ranks that we have implemented in R software version 2.13.0 (R Development Core Team 2012). Statistical analyses on the time course of $x^E(^{13}\text{C})$ in leaves and inner bark extracts were performed with R software using mixed-effect models, with tree as a random effect to estimate the effects of

time after labelling, sampling position, K fertilization and throughfall exclusion (fixed effects). Regression and covariance analyses were used to analyse linear relationships between parameters while accounting or not for treatment effects.

Results

Climate, tree growth and physiology

The 2012 dry season was unexpectedly delayed in the São Paulo state with heavy rains still occurring until the middle of June. There were, however, large differences in the amount of water stored in the first 6 m of soil between treatments during the first labelling period, with less water in $-W$ compared with $+W$ and less water in $+K$ compared with $-K$ (Figure 2). The lower amount of water stored in the soil in $+K$ than in $-K$ treatments (Figure 2b) was clearly related to much higher transpiration rates for $+K$ trees that used more water than $-K$ trees (Figure 3a). In addition, the lower water availability in $-W$ than in $+W$ may account for the lower tree transpiration under throughfall exclusion. High transpiration rates with low amount of water stored in the soil may account for lower midday leaf water potentials in $+K$ compared with $-K$ trees. Potassium fertilization significantly increased the difference between predawn and midday leaf water potentials (Table 1).

Potassium fertilization had a strong effect on tree dimension (higher circumference and height) at age 2 years, which was reflected in the size of the selected trees (Table 1). The cumulative cross-sectional growth was much higher for $+K$ than for $-K$ trees (Figure 3b). Within each K treatment, the cumulative cross-sectional growth was lower in $-W$ than in $+W$, and only the trees of the $+K-W$ treatment exhibited a marked decline in growth during the dry season.

Whole crown leaf biomass and leaf area were affected by K fertilization and, to a lesser extent, by throughfall exclusion. The CO_2 uptake by the crown was two times higher in $+K$ trees than in $-K$ trees, with no significant effect of throughfall exclusion (Table 1). Crown CO_2 uptake was well correlated with whole crown leaf biomass ($R^2 = 0.71$; $P < 0.001$, data not shown).

Temporal dynamics of ^{13}C in excess in leaves

The ^{13}C in excess in the leaves collected in the upper part of the crown, $x^E(^{13}\text{C})$, was maximal just after labelling and decreased thereafter (Figure 4a). The maximum $x^E(^{13}\text{C})$ values in leaves collected in the middle part of the crown were reached few hours after labelling (samples collected after ~ 5 h), except for the $+K+W$ treatment (Figure 4b). The same pattern was observed in leaves collected in the lower part of the crown for all treatments (Figure 4c). $x^E(^{13}\text{C})$ values decreased significantly from the top to the bottom of the crown, and the initial $x^E(^{13}\text{C})$ was higher for $+K$ trees than for $-K$ trees, but the effect of K fertilization vanished afterwards (significant interaction between fertilization and time after labelling, Table 2). In contrast,

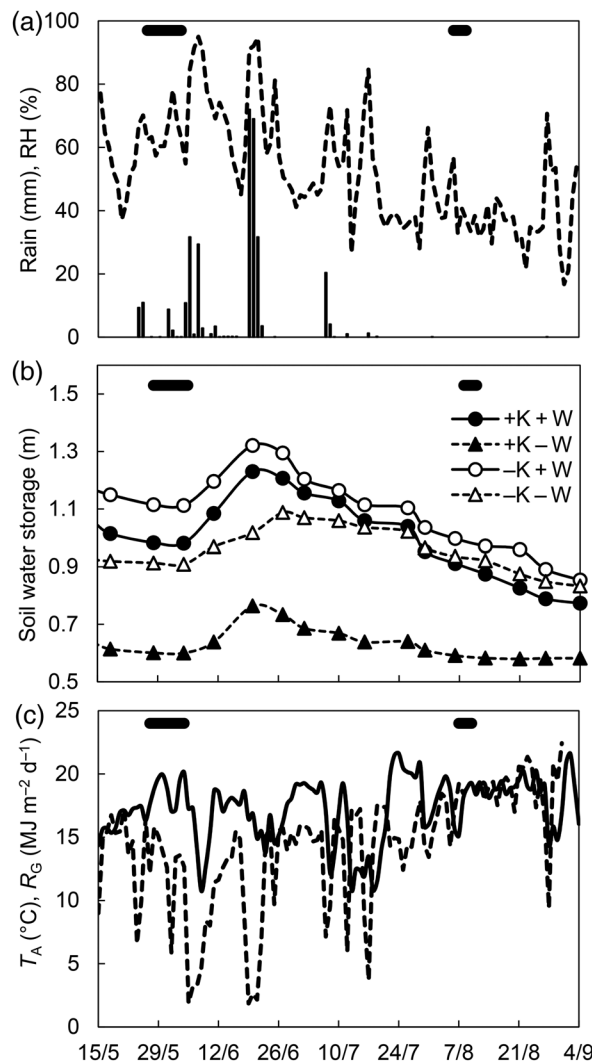


Figure 2. Time courses of (a) daily rainfall (bars) and daily minimum relative air humidity (RH, dashed line), (b) soil water stored down to a depth of 6 m in each treatment (closed symbols: $+K$, open symbols: $-K$, circles: $+W$ and triangles: $-W$) and (c) average daily air temperature (T_A , solid line) and daily global radiation (R_G , dashed line) from 15 May to 4 September 2012. The thick horizontal bars indicate the two labelling periods.

throughfall exclusion did not significantly influence the time series of leaf $x^E(^{13}\text{C})$.

The time series of $x^E(^{13}\text{C})$ in the whole crown of labelled trees (Figure 4d), modelled according to Eq. (4), revealed the existence of two significant pools of ^{13}C in the tree crown: a stabilized pool (C_S , asymptote of the curves drawn in Figure 4d) that was unaffected by the treatment and a labile pool (C_L , the portion of the curves above the asymptote in Figure 4d) that was strongly affected by the level of fertilization. C_S accounted for $<20\%$ of total ^{13}C ($C_S + C_L$) in $+K$ trees and for $25\text{--}30\%$ of total ^{13}C in $-K$ trees. C_L decreases rapidly with time with a mean residence time (τ) that was longer in $-K$ than in $+K$ trees, but not significantly because of large variations unrelated to the treatment (Table 3).

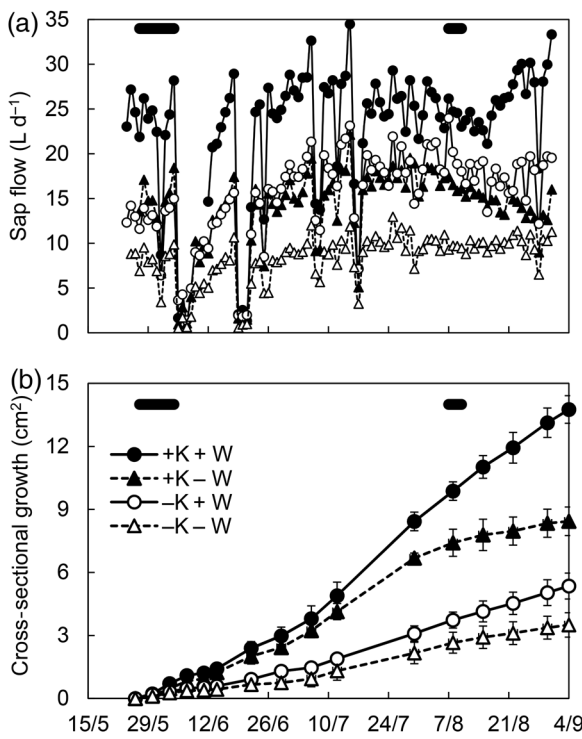


Figure 3. Time courses of (a) xylem sap flow and (b) cumulated cross-sectional area growth for three labelled trees in each treatment (closed symbols: +K, open symbols: -K, circles: +W and triangles: -W). Vertical bars are standard errors of the mean ($n = 3$). The thick horizontal bars indicate the two labelling periods. Symbols and standard error bars are omitted in (a) for clarity.

The amount of ^{13}C that was taken up by the crown during the 1-h labelling pulse ($U^{13}\text{C}$) was estimated by multiplying ($C_S + C_L$) by the leaf C content and the leaf biomass, assuming

Table 2. Probabilities (P -values) for the main effects of sampling position (P), K fertilization (F), throughfall exclusion (T) and time after labelling (D) and their interaction on $x^E(^{13}\text{C})$, the ^{13}C in excess, in leaves and inner bark extracts, using mixed-effect models with tree as a random effect (ns indicates a P -value > 0.05). Degrees of freedom (df) are given in brackets.

Factor	$x^E(^{13}\text{C})$	
	P-values [df]	
	Leaves	Inner bark extracts
Position (P)	<0.001 [2]	<0.001 [1]
K fertilization (F)	0.017 [1]	0.008 [1]
Throughfall exclusion (T)	ns [1]	ns [1]
Day after labelling (D)	<0.001 [5]	<0.001 [5]
P × F	ns [2]	0.001 [1]
P × T	ns [2]	ns [1]
F × T	ns [1]	ns [1]
P × D	<0.001 [10]	<0.001 [5]
F × D	<0.001 [5]	ns [5]
T × D	ns [5]	ns [5]
P × F × T	ns [2]	ns [1]
P × F × D	0.012 [10]	ns [5]
P × T × D	ns [10]	ns [5]
F × T × D	ns [5]	ns [5]
P × F × T × D	ns [10]	ns [5]

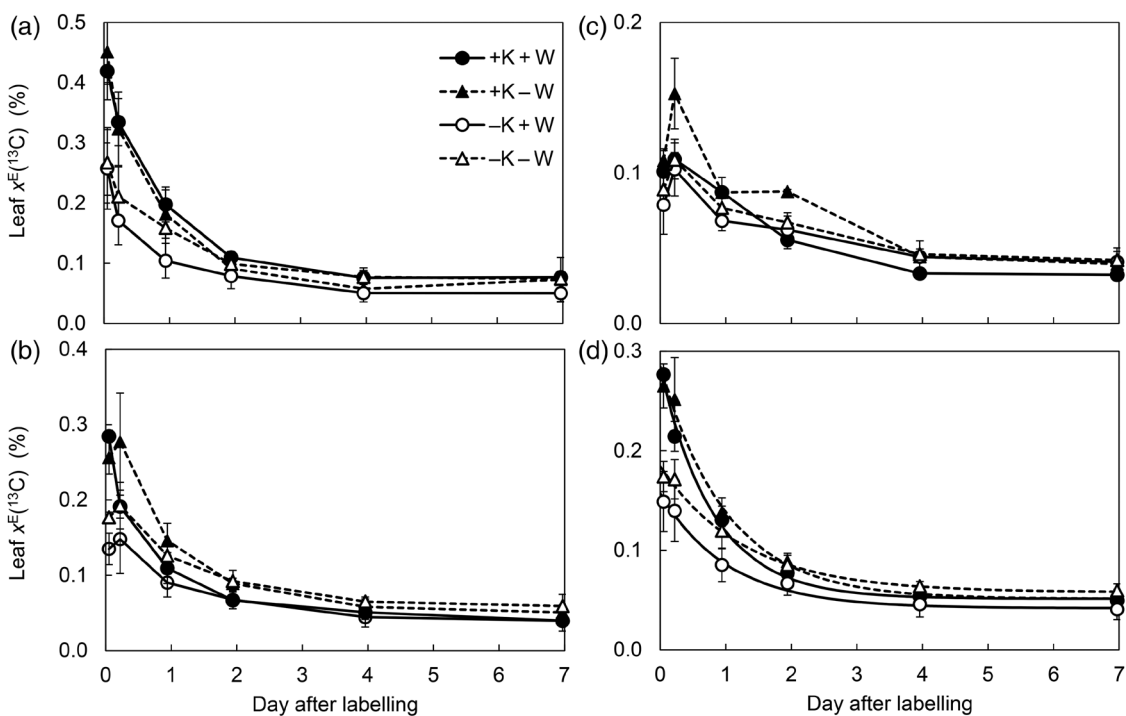


Figure 4. Time courses of $x^E(^{13}\text{C})$, the ^{13}C in excess, after pulse labelling in leaves collected in the (a) upper part, (b) middle part and (c) bottom part of the crown, and (d) calculated for the whole crown (closed symbols: +K, open symbols: -K, circles: +W, triangles: -W). Vertical bars are standard errors of the mean of three trees per treatment. In (d), the lines show the best fit of the model describing the decrease in $x^E(^{13}\text{C})$ with time after labelling. Model parameters are in Table 4.

Table 3. Model parameters describing the decrease in $x^E(^{13}\text{C})$, the ^{13}C in excess, with time after labelling in tree crown (Eq. 4). C_L is the labile pool of $x^E(^{13}\text{C})$ at time 0 and C_S is the asymptotic remaining of $x^E(^{13}\text{C})$ in the crown. τ is the mean residence time of the labile pool of $x^E(^{13}\text{C})$ in the crown, the reciprocal of rate constant of the decrease in $x^E(^{13}\text{C})$. $U^{13}\text{C}$, the total amount of ^{13}C in leaves at time 0, is the sum of C_L and C_S multiplied by the leaf C content and the leaf biomass. $U^{13}\text{C}/\tau$ is the initial rate of ^{13}C disappearance. Values are means and their standard errors for three trees per treatment. Effects of K fertilization (F), throughfall exclusion (T) and their interaction were tested using a non-parametric two-way analysis of variance based on the ranks (P-values are shown).

F	T	C_L (%)	C_S (%)	τ (h)	$U^{13}\text{C}$ (g)	$U^{13}\text{C}/\tau$ (g h $^{-1}$)
+K	+W	0.23 ± 0.02	0.05 ± 0.01	21 ± 3	5.1 ± 0.4	0.27 ± 0.08
+K	-W	0.23 ± 0.02	0.05 ± 0.00	24 ± 1	3.7 ± 0.6	0.15 ± 0.02
-K	+W	0.12 ± 0.02	0.04 ± 0.01	28 ± 8	2.0 ± 0.6	0.08 ± 0.03
-K	-W	0.13 ± 0.01	0.06 ± 0.01	31 ± 3	1.2 ± 0.1	0.04 ± 0.00
F effect		0.004	0.94	0.20	0.004	0.006
T effect		0.81	0.34	0.15	0.34	0.34
F × T		0.81	0.69	0.52	0.87	0.74

negligible losses by respiration and negligible transfer to the other tree compartments during the short labelling period. This assumption was supported by the lack of ^{13}C enrichment in inner bark extracts sampled 30 min after labelling at the base of the crown on two trees (data not shown). $U^{13}\text{C}$ ranged from 1.0 to 6.5 g, depending on the tree with a strong fertilization effect (Table 3). This amount was strongly correlated with leaf biomass ($R^2 = 0.80$) and CO_2 uptake by the crown ($R^2 = 0.88$). The difference in the amount of ^{13}C uptake reflected thus the difference in crown size and activity among trees that were mainly related to the effect of K fertilization. The initial rate of ^{13}C disappearance from the foliage, approximated by dividing $U^{13}\text{C}$ by τ , was significantly higher in +K than in -K trees, whereas the decrease due to throughfall exclusion was not significant.

^{13}C in excess in phloem sap

Although time series of $x^E(^{13}\text{C})$ in inner bark extracts did not exhibit clear treatment-specific patterns, the main result for all trees was a drop in $x^E(^{13}\text{C})$ in inner bark extracts at the bottom of the trunk, with values on average 10 times lower at the bottom of the trunk than at the base of the crown (Figure 5). The significant interaction between K fertilization and sampling position (Table 2) highlighted lower $x^E(^{13}\text{C})$ values in inner bark extracts of +K trees than -K trees at the base of the crown. The increase in $x^E(^{13}\text{C})$ was faster at the base of the crown than at the bottom of the trunk, whereas $x^E(^{13}\text{C})$ did not show any decrease during the 7-day survey except for +K +W trees.

Velocity of C transfer in the trunk

The velocity of C transfer in the trunk (V_C), estimated from the difference in time lags of recovery of ^{13}C in trunk respiration between chambers located at the base of the crown and at the bottom of the trunk, was two times higher in +K trees than in -K trees, with no significant effect of throughfall exclusion (Table 4). The bark area (A_B) of +K trees was higher than that of -K ones (Table 1). Thus, when V_C was multiplied by A_B , the difference between +K and -K trees was more pronounced (Table 4).

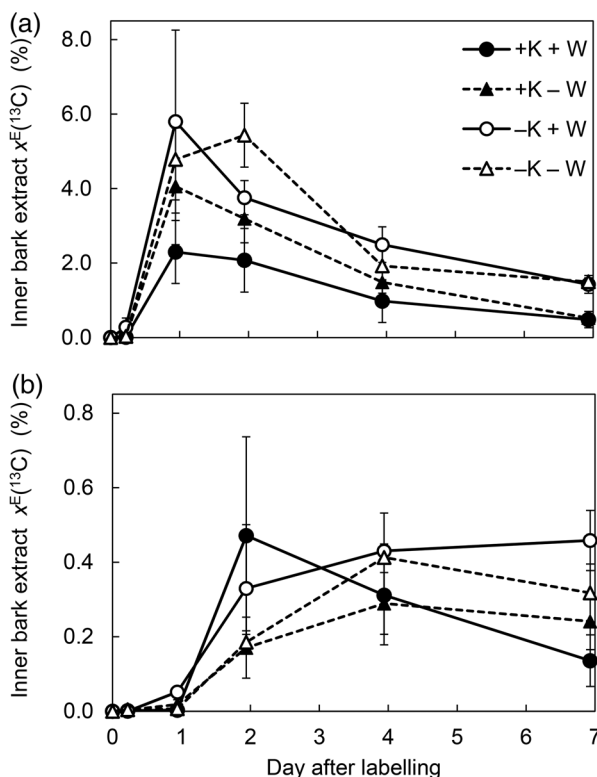


Figure 5. Time courses of $x^E(^{13}\text{C})$, the ^{13}C in excess, after pulse labelling in inner bark extracts collected at (a) the base of the crown and (b) the base of the trunk (closed symbols: +K, open symbols: -K, circles: +W and triangles: -W). Vertical bars are standard errors of the mean of three trees per treatment.

Interestingly, when V_C or $V_C \times A_B$ was plotted against crown CO_2 uptake (Figure 6), the correlation was strong when the tree from the +K -W treatment labelled in August was excluded. The time course of cross-sectional growth suggested that, for this tree, the water stress at the labelling date was much higher than that for all the other labelled trees (Figure 3b). This pattern was confirmed by midday leaf water potentials at the labelling date that ranged from -1.2 to -1.7 MPa for all the trees, except a value of -2.2 MPa for this tree.

Table 4. Velocity of C transfer in the trunk (V_C) and V_C multiplied by bark area ($V_C \times A_B$). Values are means and their standard errors for three trees per treatment. Effects of K fertilization (F), throughfall exclusion (T) and their interaction were tested using a non-parametric two-way analysis of variance based on the ranks (P -values are shown).

F	T	V_C (m h^{-1})	$V_C \times A_B$ ($\text{dm}^3 \text{h}^{-1}$)
+K	+W	0.71 ± 0.09	1.26 ± 0.14
+K	-W	0.58 ± 0.14	0.72 ± 0.18
-K	+W	0.33 ± 0.07	0.28 ± 0.06
-K	-W	0.31 ± 0.02	0.20 ± 0.03
F effect		0.02	0.004
T effect		0.42	0.34
F \times T		0.87	0.87

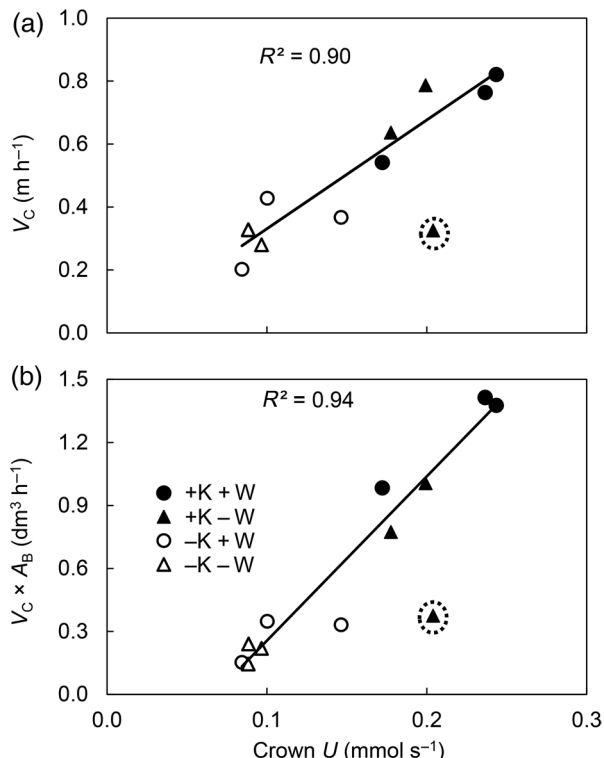


Figure 6. Relationship between net crown CO_2 uptake (crown U) and (a) the velocity of phloem transfer in the trunk (V_C) and (b) V_C multiplied by bark cross-sectional area (A_B). Closed symbols: +K, open symbols: -K, circles: +W and triangles: -W. The lines are the linear regressions (with R^2 -values) when the +K -W tree labelled in August is omitted (dotted circle).

Based on samples collected on only one tree per treatment (two trees in -K +W), the relative area of phloem element from cambium to the outer bark was 1–2% of the total inner bark area. The cross-sectional area of the sieve tubes was higher in +K trees than in -K ones, and the density of the sieve tubes was higher in +W trees than in -W ones (Table 5). The similarity between the two -K +W trees suggested a rather low variability between trees.

Time lag in root respiration

The additional time needed for labelled C to be recovered in root respiration after reaching the base of the trunk increased with

Table 5. Sieve tube density, sieve tube cross-sectional area (means and their standard errors for 53–75 sieve tubes) and sieve tube cross-sectional area relative to bark area for only one tree in each combination of K fertilization (F) and throughfall exclusion (T) treatment, except for -K +W where two trees were sampled.

F	T	Sieve tube density (mm^{-2})	Sieve tube cross-sectional area (μm^2)	Relative sieve tube cross-sectional area (%)
+K	+W	33	612 ± 34	2.1
+K	-W	25	571 ± 24	1.4
-K	+W	29	426 ± 23	1.3
		30	422 ± 43	1.3
-K	-W	21	423 ± 23	0.9

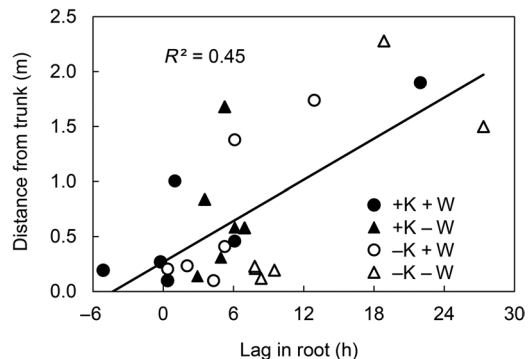


Figure 7. Lag between the onsets of the recovery of the label in the respiratory efflux at the base of the trunk (extrapolated) and in roots in relation to the distance from the trunk. Closed symbols: +K, open symbols: -K, circles: +W and triangles: -W. The line is the linear regression (with R^2 -value).

the distance from the trunk ($R^2 = 0.45$; $P < 0.001$; Figure 7). When this distance was accounted for in a covariance analysis, the time lag in root was lower in K-fertilized trees ($P = 0.015$) and higher under throughfall exclusion ($P = 0.021$). Values close to zero or even negative values were observed for chambers in the vicinity of the trunk in +K +W trees, reflecting the lack of precision in our calculation of lag differences over short distances when V_C was high. Although the velocity of C transfer in root can hardly be estimated from these data, the time required for C to run over 2 m of roots was on average three times more than that for the same distance in trunks, and thus, the velocity was three times lower.

Discussion

Uptake and fate of C in eucalypt foliage

Regardless of the treatment, the amount of ^{13}C that was taken up by the crown and recovered in leaves just after labelling was the highest in the upper part of the crown, which contained on average 46% of the total assimilated ^{13}C , and the lowest in the bottom part of the crown, which contained only 13% of the total assimilated ^{13}C . But interestingly, and in

contrast to the leaves in the upper part of the crown, the maximum $x^E(^{13}\text{C})$ values in leaves of the bottom part of the crown, and to a lesser extent in leaves of the middle part, were not reached immediately after labelling but few hours later. This suggests that leaves at the base of the crown import C that has been assimilated by leaves from the upper part for sustaining part of their energetic demand. Vertical gradients of leaf CO_2 assimilation are common in tree canopy. In addition to the decrease in light availability with depth in the crown, a decrease in the light-saturated photosynthetic rate occurs and is often related to gradients in SLA and area-based leaf nitrogen content (Ellsworth and Reich 1993, Niinemets et al. 1998), which also account for a decrease in the leaf respiration rate with depth in the crown (Lusk and Reich 2000, Meir et al. 2002, Weerasinghe et al. 2014). However, within-crown vertical variations in SLA are generally small in fast-growing eucalypt trees, much smaller than those between co-occurring small and tall trees (Nouvellon et al. 2010). Owing to the fast vertical growth of these species, it was postulated that leaves found at the bottom of the crown were produced several months before in the upper part of the crown, which can explain the lack of morphological acclimation to the low light condition that prevails deep in the canopy (Nouvellon et al. 2010, Niinemets et al. 2015). Thus, our results suggest that old leaves at the bottom of the crown may become unable to fully fulfil their own energetic requirement at least during some parts of the day when most of the light is intercepted by the upper leaves. The fact that the position of leaves changes rapidly in fast-growing trees, and thus their light status, is probably a major constraint on leaf lifespan (Ackerly 1999).

Crown CO_2 uptake did not differ between the two water supply regimes. This is consistent with the lack of effect of through-fall exclusion on stomatal conductance until end of August in 2012 (Battie-Laclau et al. 2014b), which was expected because of the deep rooting pattern of this species (Christina et al. 2011, Laclau et al. 2013) and the large amounts of water stored in deep soil layers.

The positive effects of K fertilization (+K treatments) on tree growth, crown CO_2 uptake and the amount of ^{13}C in excess recovered in leaves just after labelling are in agreement with former results on a nearby stand, showing that K fertilization increases gross primary production (GPP) and the fraction of GPP allocated to stem wood production (Epron et al. 2012b). Although variations of crown CO_2 uptake among trees were consistent with differences in the total leaf area, K fertilization also enhanced crown CO_2 uptake per unit leaf area by 36% across the two water regimes, but to a lesser extent compared with the 2.5 times higher leaf CO_2 assimilation at saturating irradiance measured by leaf gas exchange on nearby trees (Battie-Laclau et al. 2014a), which may reflect higher self-shading of leaves within larger tree crowns.

The mean residence time of labelled C in the foliage was short (21–31 h) as commonly observed (Högberg et al. 2008, Epron et al. 2012a, Warren et al. 2012), slightly shorter in K-fertilized than in K-deficient trees. Because the amount of ^{13}C in the crown immediately after labelling, and especially in the labile pool, was higher in K-fertilized trees, the initial rate of ^{13}C disappearance from the foliage was thus also higher. The disappearance of the labelled C from the foliage was due both to its use to fuel foliage respiration and to its translocation to the other tree compartments. Although the partitioning between these two processes is unknown, a higher amount of C is expected to be exported from the leaf mesophyll in K-fertilized trees than in K-deficient trees. The lower initial $x^E(^{13}\text{C})$ in inner bark extracts of +K trees than –K trees at the base of the crown may reflect a high sink strength of young, rapidly expanding leaves, which is consistent with a higher osmotically driven rate of leaf expansion in +K than in –K trees (Battie-Laclau et al. 2013).

Phloem transport and K supply

The velocity of C transfer in the trunk was about two times higher in K-fertilized trees than in K-deficient trees. This is consistent with a lower, yet not significant, mean residence time in the foliage. This is also consistent with observations made decades ago on sugarcane (Hartt 1969), tomato plant (Mengel and Viro 1974) and castor oil plant (Mengel and Haeder 1977). Potassium ions may affect the rate of phloem loading by promoting the efflux of assimilates into the apoplast prior to loading (Mengel and Haeder 1977, Doman and Geiger 1979). Although a symplastic loading mechanism has been postulated for *Eucalyptus globulus* Labill. (Merchant et al. 2010), there is no indication whether *E. grandis* is an apoplastic or a symplastic loader, but it has been suggested that passive loading is the major mechanism for tree species (Rennie and Turgeon 2009).

The fact that the linear relationship between crown CO_2 uptake and V_C or $V_C \times A_B$ did not differ between +K and –K trees suggests that the low V_C in –K trees is mainly the consequence of a lower source activity (Figure 6). In addition, the observed growth stimulation by K fertilization may also stimulate sink strength, contributing to the high V_C observed in +K trees. According to the classic Münch hypothesis, the turgor difference resulting from the loading of soluble sugars in the sieve tubes of source leaves and their unloading from the sieve tubes in sink organs drives the flow of solutes in the phloem (Van Bel 2003). However, the rate of transfer is controlled by the resistance to the flow, which mainly depends on the phloem anatomy and on the viscosity of the phloem content (Knoblauch and Peters 2010).

There was no difference in sugar concentration in the phloem sap of nearby trees across fertilization treatments (Battie-Laclau et al. 2014b). The concentration (21% w/v, on average) is close to the optimal concentration for sugar transport in plants (Jensen et al. 2013), which suggests that a difference in phloem

sap viscosity between $-K$ and $+K$ trees is unlikely to account for the difference in velocity. Lang (1983) hypothesized that K could significantly enhance the driving force for transport by increasing the turgor gradient without increasing the viscosity of the phloem sap. Hölttä et al. (2009) demonstrated theoretically that the maximum transport rate was limited by the sap viscosity and that this viscosity problem may be limited by using other solutes such as K, which would increase the turgor pressure gradient by the same amount as was the fraction of K in the phloem sap. Potassium fertilization led to a twofold increase in K concentration in phloem sap in nearby trees (Battie-Laclau et al. 2014b). However, these absolute K concentrations (12–25 mM) are several times lower than those for willow (50–300 mM, Grange and Peel 1978) or castor bean (60–90 mM, Vreugdenhil 1985), and the effect of K on the driving force depends on the relative contribution of K and its balancing anions to the total osmotic potential of the phloem sap (Thompson and Holbrook 2003a). In our case (Battie-Laclau et al. 2014b), K contributes marginally to the total osmotic potential of the phloem sap (12–25 mM compared with 21% w/v for total soluble sugars), which suggests that the higher phloem K concentration contributes only marginally to the higher velocity we observed in $+K$ compared with $-K$ trees.

Based on our observations made on only one tree per treatment, a higher resistance to sap transport is expected in the phloem of $-K$ trees due to a lower cross-sectional area of their sieve tubes (Table 5). According to the Hagen–Poiseuille equation, the resistance is a function of the diameter of the sieve element at the power of -4 . A one-third increase in sieve element cross-sectional area in response to K fertilization may thus decrease the resistance by a factor of 2 and thus increase the velocity by the same factor. The resistance does not only depend on the sieve tube dimension; part of the resistance is related to the anatomy of the sieve plate, including the number of sieve pores per sieve plate, the radius of sieve pores and the thickness of the plate (Sheehy et al. 1995, Thompson and Holbrook 2003a). However, the lumen resistance scaled with the end wall resistance across tree species, and both contribute almost equally to the total resistance (Jensen et al. 2012b, Liesche et al. 2015). The effect of environmental factors, and especially of K availability, on the anatomy of the sieve plate remains largely unexplored (Thompson 2006), but the sieve tube anatomy would probably better explain the difference in velocity than did differences in phloem sap composition and viscosity.

Regardless of the mechanism that accounts for the low V_C in $-K$ trees, it cannot be ruled out that the increase in leaf sugar concentration may partly account for the low rate of leaf photosynthesis observed in $-K$ trees (Battie-Laclau et al. 2014a) and thus that the inhibition of photosynthesis in K-deficient trees may be more the consequence than the cause of a low rate of phloem transport (Lemoine et al. 2013).

Impact of throughfall exclusion on phloem transport

There is much experimental evidence from tree seedlings that the exportation of labelled substrates from source leaves can be affected by water stress (Deng et al. 1990a, 1990b, Ruehr et al. 2009). In our study, the depressive effects of throughfall exclusion on the disappearance rate of the labelled C from the foliage and the velocity of C transfer in the trunk were not significant. Throughfall exclusion did not expose the trees labelled in June to marked water stress (predawn water potential was at -0.33 MPa for trees labelled in June in the $-W$ treatments). Such a lack of mild drought effect on phloem transport has already been reported in beech trees (Dannoura et al. 2011). Although, on average, the velocity of C transfer in the trunk was not significantly lower in $-W$ than in $+W$ trees, the value recorded for the $+K-W$ tree labelled in August was half (0.33 m h^{-1}) of that recorded for $+K-W$ trees labelled in June (0.71 m h^{-1} on average).

The volumetric flux of phloem sap (J_C), which is the product of the velocity of C transfer and the cross-sectional area of all sieve tubes, is determined at steady state by the time-integrated crown net CO_2 uptake divided by the phloem sap concentration (Hölttä et al. 2009). The fact that the $+K-W$ tree labelled in August was a clear outlier of the relation between crown CO_2 uptake and V_C or $V_C \times A_B$ (Figure 6) may indicate higher concentration of sucrose in the phloem sap, and thus an increase in sap viscosity that would have decreased the velocity. A rise in phloem sap sucrose concentration was indeed observed in August in the $+K-W$ trees of our experiment (Battie-Laclau et al. 2014b), as observed for other fast-growing eucalypt species in response to drought (Pate et al. 1998, Cernusak et al. 2003). The $+K-W$ tree labelled in August is the one that exhibited the lowest midday leaf water potential (-2.2 MPa), which confirms that the water stress was higher than that for the other labelled trees. Having additional data from trees experiencing a stronger water deficiency would, however, be required to back up these trends.

Because the xylem tissue is the source of water for the phloem tissue, assimilate transport in the phloem requires that the osmotic pressure at the phloem loading sites exceeds the drop in leaf water potential between soil and leaves due to transpiration (Nikinmaa et al. 2013, Sevanto 2014). Thus, low xylem water potential implies high osmotic pressure in the sieve tubes to attract water from the xylem, and this could be achieved by an increase in solute concentration. An increase in sugar concentration and in viscosity with water stress was recently reported in Douglas-fir trees (Woodruff 2014). The observed higher phloem sap sucrose concentration (Battie-Laclau et al. 2014b) would also increase the viscosity of the phloem sap, which would thus slow phloem transport down (Hölttä et al. 2006).

It has been suggested that solutes such as K could increase the osmotic pressure of the phloem without increasing its

viscosity (Talbott and Zeiger 1996). However, Battie-Laclau et al. (2014b) showed at our study site that the concentration of K in the phloem sap was not influenced by throughfall exclusion, which is also consistent with the lack of interaction between K fertilization and throughfall exclusion in our experiment.

The fate of assimilated C in the phloem sap

The velocity of C transfer in the trunk ranged between 0.20 and 0.82 m h⁻¹ among trees across the four treatments, which is a typical range reported for broad-leaved trees using the same approach (Dannoura et al. 2011, Epron et al. 2012a). There is still an active debate whether or not the phloem-specific conductivity and the turgor pressure differences that are commonly observed in trees can account for such a high velocity (Sevanto et al. 2003, Minchin and Lacointe 2005, Jensen et al. 2012a, Ryan and Asao 2014). It has been theoretically demonstrated that short sieve tubes in series would transport sap at a much higher velocity than a single long tube (Thompson and Holbrook 2003a, 2003b), supporting the 'relay hypothesis' introduced by Lang (1979) that assimilates are transferred from one short tube to the next one, being lost and retrieved. However, there is no experimental or anatomical evidence supporting the existence of isolated phloem segments (Murphy and Aikman 1989). Alternatively, a 'leakage-retrieval mechanism' may take place at the sieve plates along long sieve tubes (Van Bel 2003, De Schepper et al. 2013b). There is, indeed, evidence that assimilates are downloaded along the phloem pathway. This is at least needed to supply radial growth, storage and maintenance of branches, trunks and roots. However, the reloading step has been documented less (Minchin et al. 1983, Minchin and Thorpe 1987, De Schepper et al. 2013a), and its role in supporting a rapid translocation in the phloem is more controversial (Jensen et al. 2012a). As far as we know, the reloading of carbohydrate along the phloem pathway has not yet been experimentally demonstrated in field-grown trees where it is more likely to occur owing to the length of the phloem path. Our result showed that 10 times less ¹³C in excess was recovered in inner bark extracts at the bottom of the trunk when compared with the base of the crown. Because $x^E(^{13}\text{C})$ is the amount of ¹³C in excess divided by the total amount of C, this decrease suggests that a large part of the labelled assimilates has been exported out of the phloem and at least partly replaced by unlabelled soluble C containing molecules. This pattern is in agreement with the leakage-retrieval mechanism, even though further research at the scale of phloem tubes is needed to fully demonstrate it and to estimate how much of the lost C is reloaded into the phloem. Owing to the suspected role of K in the reloading of sucrose leaking from the phloem (Gajdanowicz et al. 2011), the low V_C in K-deficient trees may also result from a less efficient reloading mechanism if K channels are acting along the phloem pathways.

Conclusion

Potassium supply affects the long-distance transport of photosynthetic C in the phloem of field-grown eucalypt trees, increasing the velocity of C transfer by a factor of 2, but no clear interaction between K fertilization and drought was observed. Potassium probably has a little contribution to the turgor gradient that is driving the flow of solutes in the phloem and may not contribute to limit an increase in phloem sap viscosity under drought. However, K supply may affect the resistance to the flow of phloem sap through its impact on phloem anatomy. Owing to the growing evidence that the maintenance of phloem transport may play a central role in tree survival under drought, two major points deserve further attention: (i) how are the sieve tube and the sieve plate anatomy modulated by growth conditions such as tree nutrition and drought and how it affects phloem transport? (ii) Do sugar unloading and reloading occur along the phloem tubes, does K contribute to the efficiency of this leakage-retrieval mechanism and does this mechanism counterbalance the drought-induced change in phloem turgor pressure and avoid phloem failure related to viscosity build-up?

Acknowledgments

We are grateful to E. Araujo da Silva and the staff of Floragro (www.floragroapoio.com.br) for their technical support in the field. We also thank Rildo Moreira e Moreira and the entire staff of the Itatinga experimental station (ESALQ—USP) for their logistical support during the experiments. We also thank Shoko Tsuji for the anatomical study of phloem sample, Viviane Cristina Bettanin Maximiliano for her help in preparing samples before isotope ratio mass spectrometry analyses and Juan Sinforiano Delgado-Rojas, Marion Pilate, Elodie Merlier, Hadrien Legras, José Carlos Deus Jr and Ranieri Ribeiro for their help in the field.

Conflict of interest

None declared.

Funding

The work received financial supports from FAPESP (project 2011/09727-5). D.E. was funded by FAPESP (project 2011/23706-0) and M.D. by the Kyoto University Foundation.

References

- Ackerly D (1999) Self-shading, carbon gain and leaf dynamics: a test of alternative optimality models. *Oecologia* 119:300–310.
- Basile B, Reidel EJ, Weinbaum SA, DeJong TM (2003) Leaf potassium concentration, CO₂ exchange and light interception in almond trees (*Prunus dulcis* (Mill)). *Sci Hortic* 98:185–194.

Battie-Laclau P, Laclau J-P, Piccolo M et al. (2013) Influence of potassium and sodium nutrition on leaf area components in *Eucalyptus grandis* trees. *Plant Soil* 371:19–35.

Battie-Laclau P, Laclau J-P, Beri C et al. (2014a) Photosynthetic and anatomical responses of *Eucalyptus grandis* leaves to potassium and sodium supply in a field experiment. *Plant Cell Environ* 37:70–81.

Battie-Laclau P, Laclau J-P, Domec J-C et al. (2014b) Effects of potassium and sodium supply on drought-adaptive mechanisms in *Eucalyptus grandis* plantations. *New Phytol* 203:401–413.

Berkowitz GA, Whalen C (1985) Leaf K⁺ interaction with water stress inhibition of nonstomatal-controlled photosynthesis. *Plant Physiol* 79:189–193.

Cakmak I (2010) Potassium for better crop production and quality. *Plant Soil* 335:1–2.

Cernusak LA, Arthur DJ, Pate JS, Farquhar GD (2003) Water relations link carbon and oxygen isotope discrimination to phloem sap sugar concentration in *Eucalyptus globulus*. *Plant Physiol* 131:1544–1554.

Christina M, Laclau J-P, Gonçalves JLM, Jourdan C, Nouvellon Y, Bouillet J-P (2011) Almost symmetrical vertical growth rates above and below ground in one of the world's most productive forests. *Ecosphere* 2:art27. doi:10.1890/ES10-00158.1

Christina M, Le Maire G, Battie-Laclau P, Nouvellon Y, Bouillet JP, Jourdan C, de Moraes Goncalves JL, Laclau JP (2015) Measured and modeled interactive effects of potassium deficiency and water deficit on gross primary productivity and light-use efficiency in *Eucalyptus grandis* plantations. *Glob Change Biol* 21:2022–2039.

Cobo JG, Dercon G, Cadisch G (2010) Nutrient balances in African land use systems across different spatial scales: a review of approaches, challenges and progress. *Agric Ecosyst Environ* 136:1–15.

Coplen TB (2011) Guidelines and recommended terms for expression of stable-isotope-ratio and gas-ratio measurement results. *Rapid Commun Mass Spectrom* 25:2538–2560.

Dannoura M, Kominami Y, Tamai K, Jomura M, Miyama T, Goto Y, Kanazawa Y (2006) Development of an automatic chamber system for long-term measurements of CO₂ flux from roots. *Tellus B* 58:502–512.

Dannoura M, Maillard P, Fresneau C et al. (2011) In situ assessment of the velocity of carbon transfer by tracing ¹³C in trunk CO₂ efflux after pulse labelling: variations among tree species and seasons. *New Phytol* 190:181–192.

Deng X, Joly RJ, Hahn DT (1990a) The influence of plant water deficit on distribution of ¹⁴C-labelled assimilates in cacao seedlings. *Ann Bot* 66:211–217.

Deng X, Joly RJ, Hahn DT (1990b) The influence of plant water deficit on photosynthesis and translocation of ¹⁴C-labeled assimilates in cacao seedlings. *Physiol Plant* 78:623–627.

De Schepper V, Bühler J, Thorpe M, Roeb G, Huber G, van Dusschoten D, Jahnke S, Steppe K (2013a) ¹¹C-PET imaging reveals transport dynamics and sectorial plasticity of oak phloem after girdling. *Front Plant Sci* 4:200.

De Schepper V, De Swaef T, Bauweraerts I, Steppe K (2013b) Phloem transport: a review of mechanisms and controls. *J Exp Bot* 64:4839–4850.

Doman DC, Geiger DR (1979) Effect of exogenously supplied foliar potassium on phloem loading in *Beta vulgaris* L. *Plant Physiol* 64:528–533.

Ellsworth DS, Reich PB (1993) Canopy structure and vertical patterns of photosynthesis and related leaf traits in a deciduous forest. *Oecologia* 96:169–178.

Epron D, Bahn M, Derrien D et al. (2012a) Pulse-labelling trees to study carbon allocation dynamics: a review of methods, current knowledge and future prospects. *Tree Physiol* 32:776–798.

Epron D, Laclau J-P, Almeida JCR, Gonçalves JLM, Ponton S, Sette CR, Delgado-Rojas JS, Bouillet J-P, Nouvellon Y (2012b) Do changes in carbon allocation account for the growth response to potassium and sodium applications in tropical *Eucalyptus* plantations? *Tree Physiol* 32:667–679.

Fatichi S, Leuzinger S, Körner C (2014) Moving beyond photosynthesis: from carbon source to sink-driven vegetation modeling. *New Phytol* 201:1086–1095.

Fischer RA (1968) Stomatal opening: role of potassium uptake by guard cells. *Science* 160:784–785.

Fromm J (2010) Wood formation of trees in relation to potassium and calcium nutrition. *Tree Physiol* 30:1140–1147.

Gajdanowicz P, Michard E, Sandmann M et al. (2011) Potassium (K⁺) gradients serve as a mobile energy source in plant vascular tissues. *Proc Natl Acad Sci USA* 108:864–869.

Grange RL, Peel AJ (1978) Evidence for solution flow in the phloem of willow. *Planta* 138:15–23.

Granier A (1985) Une nouvelle méthode pour la mesure du flux de sève brute dans le tronc des arbres. *Ann For Sci* 42:193–200.

Hartt CE (1969) Effect of potassium deficiency upon translocation of ¹⁴C in attached blades and entire plants of sugarcane. *Plant Physiol* 44:1461–1469.

Hartt CE (1970) Effect of potassium deficiency upon translocation of ¹⁴C in detached blades of sugarcane. *Plant Physiol* 45:183–187.

Högberg P, Högberg MN, Göttlicher SG et al. (2008) High temporal resolution tracing of photosynthate carbon from the tree canopy to forest soil microorganisms. *New Phytol* 177:220–228.

Hölttä T, Vesala T, Sevanto S, Perämäki M, Nikinmaa E (2006) Modeling xylem and phloem water flows in trees according to cohesion theory and Münch hypothesis. *Trees* 20:67–78.

Hölttä T, Mencuccini M, Nikinmaa E (2009) Linking phloem function to structure: analysis with a coupled xylem–phloem transport model. *J Theor Biol* 259:325–337.

Jensen KH, Liesche J, Bohr T, Schulz A (2012a) Universality of phloem transport in seed plants. *Plant Cell Environ* 35:1065–1076.

Jensen KH, Mullendore DL, Holbrook NM, Bohr T, Knoblauch M, Bruus H (2012b) Modeling the hydrodynamics of phloem sieve plates. *Front Plant Sci* 3:151.

Jensen KH, Savage JA, Holbrook NM (2013) Optimal concentration for sugar transport in plants. *J R Soc Interface* 10:20130055.

Jin SH, Huang JQ, Li XQ, Zheng BS, Wu JS, Wang ZJ, Liu GH, Chen M (2011) Effects of potassium supply on limitations of photosynthesis by mesophyll diffusion conductance in *Carya cathayensis*. *Tree Physiol* 31:1142–1151.

Keeling CD (1958) The concentration and isotopic abundances of atmospheric carbon dioxide in rural areas. *Geochim Cosmochim Acta* 13:322–334.

Knoblauch M, Peters WS (2010) Münch, morphology, microfluidics—our structural problem with the phloem. *Plant Cell Environ* 33: 1439–1452.

Laclau JP, Almeida JCR, Gonçalves JLM, Saint-André L, Ventura M, Ranger J, Moreira RM, Nouvellon Y (2009) Influence of nitrogen and potassium fertilization on leaf lifespan and allocation of above-ground growth in *Eucalyptus* plantations. *Tree Physiol* 29:111–124.

Laclau J-P, Ranger J, de Moraes Gonçalves JL et al. (2010) Biogeochemical cycles of nutrients in tropical *Eucalyptus* plantations: main features shown by intensive monitoring in Congo and Brazil. *For Ecol Manag* 259:1771–1785.

Laclau J-P, da Silva EA, Rodrigues Lambais G et al. (2013) Dynamics of soil exploration by fine roots down to a depth of 10 m throughout the entire rotation in *Eucalyptus grandis* plantations. *Front Plant Sci* 4:243.

Lang A (1979) A relay mechanism for phloem translocation. *Ann Bot* 44:141–145.

Lang A (1983) Turgor-regulated translocation. *Plant Cell Environ* 6:683–689.

Lemoine R, La Camera S, Atanassova R et al. (2013) Source-to-sink transport of sugar and regulation by environmental factors. *Front Plant Sci* 4:272.

Liesche J, Windt C, Bohr T, Schulz A, Jensen KH (2015) Slower phloem transport in gymnosperm trees can be attributed to higher sieve element resistance. *Tree Physiol* 35:376–386.

Lusk CH, Reich PB (2000) Relationships of leaf dark respiration with light environment and tissue nitrogen content in juveniles of 11 cold-temperate tree species. *Oecologia* 123:318–329.

Meir P, Kruijt B, Broadmeadow M, Barbosa E, Kull O, Carswell F, Nobre A, Jarvis PG (2002) Acclimation of photosynthetic capacity to irradiance in tree canopies in relation to leaf nitrogen concentration and leaf mass per unit area. *Plant Cell Environ* 25:343–357.

Mengel K, Haeder H-E (1977) Effect of potassium supply on the rate of phloem sap exudation and the composition of phloem sap of *Ricinus communis*. *Plant Physiol* 59:282–284.

Mengel K, Viro M (1974) Effect of potassium supply on the transport of photosynthates to the fruits of tomatoes (*Lycopersicon esculentum*). *Physiol Plant* 30:295–300.

Merchant A, Tausz M, Keitel C, Adams MA (2010) Relations of sugar composition and $\delta^{13}\text{C}$ in phloem sap to growth and physiological performance of *Eucalyptus globulus* (Labill.). *Plant Cell Environ* 33:1361–1368.

Minchin PEH, Lacointe A (2005) New understanding on phloem physiology and possible consequences for modelling long-distance carbon transport. *New Phytol* 166:771–779.

Minchin PEH, Thorpe MR (1987) Measurement of unloading and reloading of photo-assimilate within the stem of bean. *J Exp Bot* 38:211–220.

Minchin PEH, Lang A, Thorpe MR (1983) Dynamics of cold induced inhibition of phloem transport. *J Exp Bot* 34:156–162.

Murphy R, Aikman DP (1989) An investigation of the relay hypothesis of phloem transport in *Ricinus communis* L. *J Exp Bot* 40:1079–1088.

Nardini A, Dimasi F, Klepsch M, Jansen S (2012) Ion-mediated enhancement of xylem hydraulic conductivity in four *Acer* species: relationships with ecological and anatomical features. *Tree Physiol* 32:1434–1441.

Niinemets Ü, Kull O, Tenhunen JD (1998) An analysis of light effects on foliar morphology, physiology, and light interception in temperate deciduous woody species of contrasting shade tolerance. *Tree Physiol* 18:681–696.

Niinemets Ü, Keenan TF, Hallik L (2015) A worldwide analysis of within-canopy variations in leaf structural, chemical and physiological traits across plant functional types. *New Phytol* 205:973–993.

Nikinmaa E, Hölttä T, Hari P, Kolari P, Mäkelä A, Sevanto S, Vesala T (2013) Assimilate transport in phloem sets conditions for leaf gas exchange. *Plant Cell Environ* 36:655–669.

Nikinmaa E, Sievanen R, Holtta T (2014) Dynamics of leaf gas exchange, xylem and phloem transport, water potential and carbohydrate concentration in a realistic 3-D model tree crown. *Ann Bot* 114:653–666.

Nouvelon Y, Laclau J-P, Epron D et al. (2010) Within-stand and seasonal variations of specific leaf area in a clonal *Eucalyptus* plantation in the Republic of Congo. *For Ecol Manag* 259:1796–1807.

Oddo E, Inzerillo S, La Bella F, Grisafi F, Salleo S, Nardini A (2011) Short-term effects of potassium fertilization on the hydraulic conductance of *Laurus nobilis* L. *Tree Physiol* 31:131–138.

Oddo E, Inzerillo S, Grisafi F, Sajeva M, Salleo S, Nardini A (2014) Does short-term potassium fertilization improve recovery from drought stress in laurel? *Tree Physiol* 34:906–913.

Pate J, Shedley E, Arthur D, Adams M (1998) Spatial and temporal variations in phloem sap composition of plantation-grown *Eucalyptus globulus*. *Oecologia* 117:312–322.

Pettigrew WT (2008) Potassium influences on yield and quality production for maize, wheat, soybean and cotton. *Physiol Plant* 133:670–681.

Pier PA, Berkowitz GA (1987) Modulation of water stress effects on photosynthesis by altered leaf K^+ . *Plant Physiol* 85:655–661.

R Development Core Team (2012) R: a language and environment for statistical computing. R Foundation for Statistical Computing, Vienna, Austria. www.r-project.org.

Rennie EA, Turgeon R (2009) A comprehensive picture of phloem loading strategies. *Proc Natl Acad Sci USA* 106:14162–14167.

Robin C, Shamsun-Noor L, Guckert A (1989) Effect of potassium on the tolerance to PEG-induced water stress of two white clover varieties (*Trifolium repens* L.). *Plant Soil* 120:153–158.

Roelfsema MRG, Hedrich R (2005) In the light of stomatal opening: new insights into 'the Watergate'. *New Phytol* 167:665–691.

Römhild V, Kirkby EA (2010) Research on potassium in agriculture: needs and prospects. *Plant Soil* 335:155–180.

Ruehr NK, Offermann CA, Gessler A, Winkler JB, Ferrio JP, Buchmann N, Barnard RL (2009) Drought effects on allocation of recent carbon: from beech leaves to soil CO_2 efflux. *New Phytol* 184:950–961.

Ryan MG, Asao S (2014) Phloem transport in trees. *Tree Physiol* 34:1–4.

Santiago LS, Wright SJ, Harms KE, Yavitt JB, Korine C, Garcia MN, Turner BL (2012) Tropical tree seedling growth responses to nitrogen, phosphorus and potassium addition. *J Ecol* 100:309–316.

Sardans J, Peñuelas J (2015) Potassium: a neglected nutrient in global change. *Glob Ecol Biogeogr* 24:261–275.

Sevanto S (2014) Phloem transport and drought. *J Exp Bot* 65: 1751–1759.

Sevanto S, Vesala T, Perämäki M, Nikinmaa E (2003) Sugar transport together with environmental conditions controls time lags between xylem and stem diameter changes. *Plant Cell Environ* 26: 1257–1265.

Shabala S, Pottosin I (2014) Regulation of potassium transport in plants under hostile conditions: implications for abiotic and biotic stress tolerance. *Physiol Plant* 151:257–279.

Shabala SN, Lew RR (2002) Turgor regulation in osmotically stressed *Arabidopsis* epidermal root cells. Direct support for the role of inorganic ion uptake as revealed by concurrent flux and cell turgor measurements. *Plant Physiol* 129:290–299.

Sheehy JE, Mitchell PL, Durand J-L, Gastal F, Woodward FI (1995) Calculation of translocation coefficients from phloem anatomy for use in crop models. *Ann Bot* 76:263–269.

Smethurst P, Knowles A, Churchill K, Wilkinson A, Lyons A (2007) Soil and foliar chemistry associated with potassium deficiency in *Pinus radiata*. *Can J For Res* 37:1093–1105.

Sokal RR, Rohlf FJ (1995) Biometry. W. H. Freeman, New-York, USA, p 887.

Stroock AD, Pagay VV, Zwieniecki MA, Michele Holbrook N (2014) The physicochemical hydrodynamics of vascular plants. *Annu Rev Fluid Mech* 46:615–642.

Sung FJM, Krieg DR (1979) Relative sensitivity of photosynthetic assimilation and translocation of 14 carbon to water stress. *Plant Physiol* 64:852–856.

Talbott LD, Zeiger E (1996) Central roles for potassium and sucrose in guard-cell osmoregulation. *Plant Physiol* 111:1051–1057.

Taulya G (2013) East African highland bananas (*Musa* spp. AAA-EA) 'worry' more about potassium deficiency than drought stress. *Field Crops Res* 151:45–55.

Thompson MV (2006) Phloem: the long and the short of it. *Trends Plant Sci* 11:26–32.

Thompson MV, Holbrook NM (2003a) Application of a single-solute non-steady-state phloem model to the study of long-distance assimilate transport. *J Theor Biol* 220:419–455.

Thompson MV, Holbrook NM (2003b) Scaling phloem transport: water potential equilibrium and osmoregulatory flow. *Plant Cell Environ* 26:1561–1577.

Triboulou M-B, Pritchard J, Levy G (1997) Effects of potassium deficiency on cell water relations and elongation of tap and lateral roots of maritime pine seedlings. *New Phytol* 135:183–190.

Trifilò P, Nardini A, Raimondo F, Lo Gullo MA, Salleo S (2011) Ion-mediated compensation for drought-induced loss of xylem hydraulic conductivity in field-growing plants of *Laurus nobilis*. *Funct Plant Biol* 38:606–613.

Tripler CE, Kaushal SS, Likens GE, Todd Walter M (2006) Patterns in potassium dynamics in forest ecosystems. *Ecol Lett* 9: 451–466.

Van Bel AJE (2003) The phloem, a miracle of ingenuity. *Plant Cell Environ* 26:125–149.

Vreugdenhil D (1985) Source-to-sink gradient of potassium in the phloem. *Planta* 163:238–240.

Warren JM, Iversen CM, Garten CT et al. (2012) Timing and magnitude of C partitioning through a young loblolly pine (*Pinus taeda* L.) stand using ^{13}C labeling and shade treatments. *Tree Physiol* 32:799–813.

Weerasinghe LK, Creek D, Crous KY, Xiang S, Liddell MJ, Turnbull MH, Atkin OK (2014) Canopy position affects the relationships between leaf respiration and associated traits in a tropical rainforest in Far North Queensland. *Tree Physiol* 34:564–584.

Wind C, Arend M, Fromm J (2004) Potassium-dependent cambial growth in poplar. *Plant Biol* 6:30–37.

Woodruff DR (2014) The impacts of water stress on phloem transport in Douglas-fir trees. *Tree Physiol* 34:5–14.

Wright SJ, Yavitt JB, Wurzburger N et al. (2011) Potassium, phosphorus, or nitrogen limit root allocation, tree growth, or litter production in a lowland tropical forest. *Ecology* 92:1616–1625.